Design of an Arm Exoskeleton with Scapula Motion for Shoulder Rehabilitation

Craig Carignan
Imaging Science and Information Systems (ISIS) Center
Department of Radiology
Georgetown University
Washington, DC 20057
Email: crc32@georgetown.edu

Michael Liszka
Stephen Roderick
Space Systems Laboratory (SSL)
Department of Aerospace Engineering
University of Maryland
College Park, MD 20742
Email: liszka@ssl.umd.edu, roderick@ssl.umd.edu

***Abstract*— The evolution of an arm exoskeleton design for treating shoulder pathology is examined. Tradeoffs between various kinematics configurations are explored, and a device with five active degrees of freedom is proposed. Two rapid-prototype designs were built and fitted to several subjects to verify the kinematic design and determine passive link adjustments. Control modes are developed for exercise therapy and functional rehabilitation, and a distributed software architecture that incorporates computer safety monitoring is described. Although intended primarily for therapy, the exoskeleton will also be used to monitor progress in strength, range of motion, and functional task performance.**

I. INTRODUCTION

The development of robotic exoskeletons for physical therapy is relatively recent in the field of robotics. Powered orthotic devices have been in use for over a decade, but the focus of these mechanisms has been assistive rather than rehabilitative. The primary role of exoskeletons thus far has been as a haptic device for virtual reality (VR) applications. Prime examples of these devices include the portable, back-mounted *EXOS Force ArmMaster* and the floor-mounted *FREFLEX Exoskeleton* [4].

When designing portable exoskeletons, the classic tradeoff between power and weight always emerges. VR exoskeletons are almost always motor-driven in order to attain the high control bandwidths required for simulating contact with virtual environments. Unfortunately, motors have very low power-to-weight ratios, which tend to limit the force output of the exoskeleton for physical therapy application. Pneumatic-actuators, on the other hand, have high power-to-weight ratios but poor actuator response, rendering them too bandwidth-limited for functional rehabilitation.

This work builds upon advances in actuator/drive technology to develop a lightweight but powerful exoskeleton that can be used for exercise therapy and functional rehabilitation. The article begins with a brief survey of previous arm exoskeletons in Section II. The kinematic and mechanical designs are discussed in Section III. The exoskeleton control system and operational modes are discussed in Section IV. The software architecture and safety system are addressed in Section V. Some conclusions are observed in Section VI, and the status of the exoskeleton development is reviewed.

II. PREVIOUS WORK

In order to closely follow the motion of the human arm, exoskeletons are typically designed with the seven principal degrees of freedom (DOF) of the human arm: shoulder (3), elbow (1), and wrist (3). The sequence of rotations shown in Figure 1 reflects the convention commonly used in the biomechanics community [18]. The glenohumeral (GH) joint is modeled as a 3-DOF ball and socket joint defined by a set of rotating coordinates. The first joint, shoulder flexion/extension, is defined as the rotation of the shoulder about an axis through the GH joint and perpendicular to the longitudinal body axis. The second axis, shoulder abduction/adduction, is the rotation of the upper arm toward/away from the body about an axis that is perpendicular to the flexion axis and the longitudinal axis through the upper arm. The third axis, shoulder medial/lateral (internal/external) rotation, is the roll about the longitudinal axis of the upper arm. Note that this GH model is purely rotational; it does not include translation of the glenohumeral joint caused by scapulothoracic motion, clavicle rotation, and other joints in the shoulder [13].

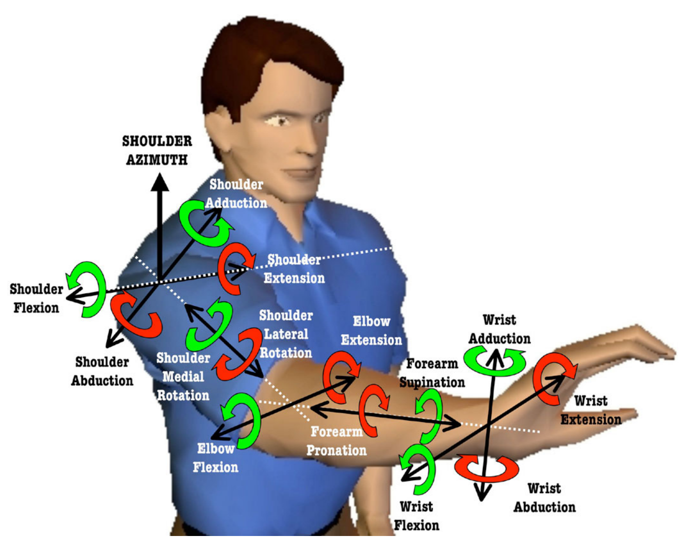

Fig. 1. The seven principal degrees of freedom of the human arm (adapted from [18]).

Alternatively, several bioengineering researchers have favored the "azimuth-elevation-roll" convention commonly used in scientific practice [23]. In this standard, the first shoulder rotation, "azimuth," is the rotation about a vertical axis through the shoulder. The second rotation, "elevation," is rotation of the upper arm about an axis orthogonal to both the azimuth axis and the longitudinal axis of the upper arm. The third shoulder axis, "roll," is the rotation of the upper arm about its longitudinal axis and is the same as the "shoulder" rotation in the biomechanics convention.

Several of the arm exoskeleton prototypes that have been built to-date are listed in Table I. The table lists the number of joints, power source, mass, upper/forearm lengths, and the shoulder type. If the exoskeleton is portable, then the mass of the backpack and exoskeleton are each given. The two lengths reported are for the upper arm and forearm links. Four different shoulder types appear based upon the sequence of rotations in the shoulder. The range of motion and continuous static torques for several of these devices are listed in Table II and Table III.

The majority of exoskeletons listed in Table I were developed as haptic devices for virtual reality (VR) applications. Haptic devices are typically driven by motors to provide the high control bandwidth required for interaction with virtual environments and thus have relatively low power output as seen in Table III. The only exoskeleton that even comes close to human output capability is the hydraulically-powered *Sarcos Dextrous Arm Master* developed as a force-reflecting master arm for teleoperation applications [11]. While this may be the most powerful exoskeleton, it is also the heaviest.

TABLE I

ARM EXOSKELETON PROTOTYPES.

DEVICE	DOF #	Port? Y/N	Power *	Mass† (kg)	Length‡ (cm)	Type $\triangle$
EXOS [4]	5	Y	E	8.2/1.8	?/?	FAR
Dex [11]	7	N	H	20.9	31.1/25.9	FAR
Sensor [21]	7	N	E	6	24.0/28.5	FAR
GIA [2], [16]	5	N	E	10	30.5/25.0	AFR
ATHD [8]	7	Y	E	?/2.3	?/?	BSR
MB [22]	7	Y	∅	?/15	28.3/26.5	ZLR
FreFlex [10]	7	N	E	?	37.2/29.9	AFR
pMA [25]	7	N	P	2	?/?	FAR
Salford [5]	9	Y	∅	?/0.75	?/?	AFR
MULOS [12]	5	N	E	2	?/?	ZLR
UWash [24]	7	N	E	?	?/?	AFR

* E-electric, H-hydraulic, P-pneumatic, ∅-unactuated
† Backpack/Arm (from first GH joint)
‡ Upper Arm (GH to Elbow)/Forearm (Elbow to Wrist)
$^{\triangle}$ FAR (flexion-abduction-rotation), AFR (abduction-flexion-rotation), ZLR (azimuth-elevation-roll), BSR (ball&socket-rotation)

A number of unactuated devices have also been built for gathering anthropomorphic data such as the *MB Exoskeleton* developed for the U.S. Air Force and shown in Figure 2 [22]. Although this device is passive, it incorporated a number of features important for physiotherapy applications such as good range of motion, adjustable link lengths (±2.5 cm upper arm, ±2.0 cm forearm), and portability. The project was discontinued before a powered exoskeleton was built, but first-hand observation provided a lot of valuable information.

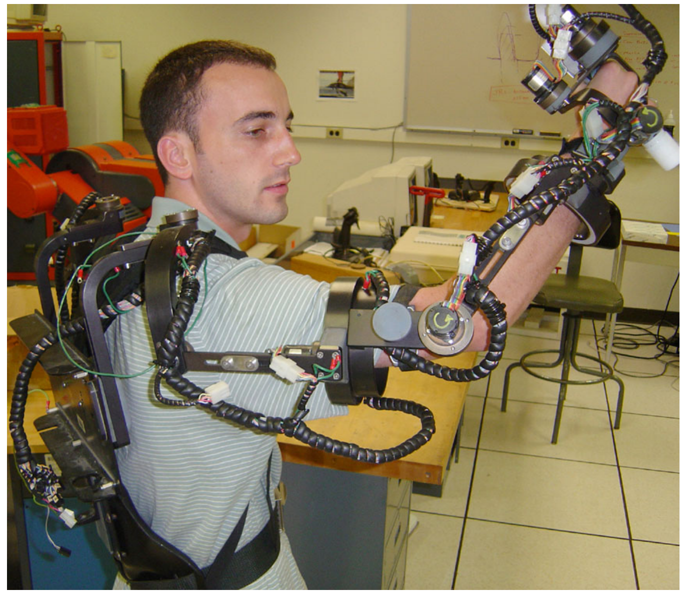

Fig. 2. SSL personnel dons the MB Exoskeleton during visit to Wright-Patterson Air Force Base. (SSL Photo Archives – used with permission of the Wright-Patterson Air Force Research Laboratory)

The tradeoff between power-to-weight ratio and control bandwidth for haptic devices has been addressed by several researchers [4]. Recent articles suggest a trend toward using pneumatically powered exoskeletons for physical therapy. Examples of these include the *pMA Exoskeleton* which utilizes pneumatic muscle actuators (pMA) [25] and the *Skil Mate* wearable elbow/forearm exoskeleton powered by McKibben artificial muscles [26] and developed for astronaut extravehicular activity (EVA). While these devices have excellent power-to-weight ratios, they have relatively low bandwidth capability ($\approx 0.5Hz$), making them poorly suited at present for virtual reality applications. However, they do show excellent promise as assistive and resistive training devices.

The Motorized Upper Limb Orthotic System (*MULOS*) is a wheelchair-mounted exoskeleton developed for use by persons with weak upper limbs [12]; thus, it is not intended as an exercise system for fit adults. In addition, there is no compensation for scapulo-thoracic motion, which is considered key for shoulder rehabilitation. Nonetheless, *MULOS* provided some valuable guidelines for designing the shoulder kinematics as well as instituting a number of novel safety features, such as a slip clutch for protection against spastic motions.

The only exoskeleton that has explicitly allowed for scapulothoracic motion is the non-driven *Salford ArmMaster* developed for tactile VR applications [5], [6]. This exoskeleton incorporates scapula tilt of up to 60° and scapula medial rotation of up to 45° that could generate up to 12 cm of scapula elevation/depression. *MULOS* researchers examined the translation of the GH joint for several assistive tasks and deemed that the motion was not critical in their application [3]. The Japanese-designed *ATHD* has used flex cables to drive the shoulder rotational degrees of freedom from motors mounted in a backpack, an approach that could allow for motion of the GH-joint, but only at the expense of shoulder rotation.

TABLE II
EXOSKELETON JOINT RANGES OF MOTION (DEG).

JOINT	Man [18]†	Exos [4]	Dex [4]	Fre [10]	GIA [2]	Sen [20]	HD [8]	MB [22]
shoulder flex/ext	188 /61	120	180	130 /52	55 /36	150 /30	180 /50	130
shoulder abd/add	134 /48	120	180	28 /18	73 /73	50 /0	180 /0	135
shoulder med/lat	97 /34	100	180	90 /90	77 /81	60 /60	90 /90	260
elbow flex/ext	142 /0	100	105	166 /-3	89 /15	90 /0	115 /0	135
forearm pro/sup	85 /90	100	105	90 /90	99 /88	90 /90	90 /90	215
wrist flex/ext	90 /99	–	180	38 /39	50 /20	60 /60	70 /90	90
wrist abd/add	47 /27	–	100	57 /52	80 /80	15 /15	55 /25	30

†Mean values for dominant arm of 39 males

TABLE III
EXOSKELETON MAXIMUM JOINT TORQUES (N-M).

JOINT	Human [9]† [1]‡	Exos [4]	Dex [4]	Fre [10]	GIA [16]	pMA [25]
shoulder flex/ext	115 /110	6.4	97	34	20	30
shoulder abd/add	134 /94	6.4	97	34	20	27
shoulder med/lat	–	2.3	50	17	10	6
elbow flex/ext	72.5 /42.1	1.6	50	17	10	6
forearm sup/pro	9.1 /7.3	0.4	50	5.6	2	5
wrist flex/ext	19.8 /10.2	–	5.5	2.8	–	4
wrist abd/add	20.8 /17.8	–	5.5	2.8	–	4

†Mean values for male shoulder, dominant arm
‡Mean values for male elbow/wrist, dominant arm

III. MECHANICAL DESIGN

A driving goal for the Maryland-Georgetown-Army (MGA) Exoskeleton was to use the lowest number of DOFs possible to allow for full exercise therapy of the shoulder complex. Considering the design from a biomechanical perspective, it was determined that five powered degrees of freedom would be required. Based on first hand experience of several physical therapists, allowing for incidental or deliberate motion of the scapulothoracic joint would be critical to achieving our goals so a scapula joint was included in the design. Three joints would be required for glenohumural shoulder rotation. An elbow joint was needed since several flexion/extension muscles (triceps and biceps brachii) are articulated through the shoulder [13]. The inclusion of the elbow implied the addition of a forearm linkage, so the forearm roll was added as a passive joint. The following sections will review the development of the kinematics, construction of the rapid-prototypes, and selection of the hardware.

A. Kinematics

Two major issues arose in the design of the exoskeleton: how to articulate translation of the shoulder joint and where to place the shoulder singularity. It was clear that designing a device to fully articulate 11 or more DOFs of the shoulder complex would not be reasonable [19], so our goal was to use a single rotary joint as a first order approximation of shoulder translation. In addition, the singularity or "gimbal lock" that results from using three single-axis shoulder joints had to be addressed. The intent was to place the singularity at an azimuth and elevation that would be least likely to interfere with rehabilitation tasks.

Since our goal was to capture as much of the scapulothoracic motion as possible using a single rotary joint, we decided to focus on the largest motion, which is shoulder elevation and depression. Shoulder elevation can occur either deliberately, e.g. shoulder shrug, or incidentally during rotation of the glenohumeral (GH) joint. An example of the latter occurs during shoulder abduction starting from the arm hanging straight down by the side of the leg and moving in a circular arc above the head like in a jumping jack motion.

Figure 3 shows the translation of the GH joint in the frontal plane and was generated by using video capture data from a shoulder abduction movement [19]. The vertical displacement (elevation) of the shoulder was found to be far greater than the horizontal (protraction) displacement, with a sharp point in the curve where the adduction angle reaches 90° (arm is horizontal). This point corresponds to the onset of rotation of the clavicle, which then thrusts the acromio-clavicular (AC) joint and consequently the GH joint as the shoulder continues to elevate.

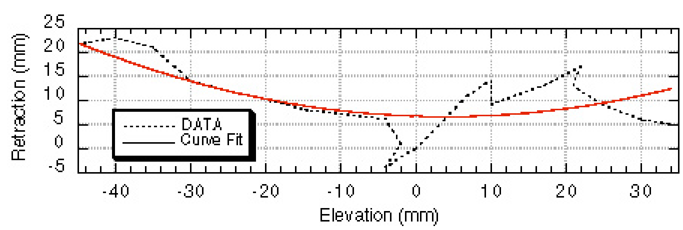

Fig. 3. Displacement of shoulder in frontal plane during a 180° shoulder abduction using data taken from [19] (curve fit is 2nd order polynomial).

If a circular curve could be fit to data similar to Figure 3, an axis of rotation could be identified for placement of a scapulothoracic joint. Since the axis of this joint is perpendicular to the frontal plane, it could be mounted anywhere along a line normal to the back. Therefore, the motor can be conveniently mounted on a backpack strapped to the subject's torso and can yield the desired elevation and depression of the shoulder joint.

Shoulder singularities were the second major issue to be confronted. The GH joint is usually modeled kinematically as a ball and socket joint. However, attempting to implement the same type of joint in the exoskeleton would pose severe design challenges as well as introduce interference between the human joint and robotic joint. Instead, the ball and socket joint is replaced by three serially connected pin joints. Although the pin joints create three DOFs around a single point, they do not exactly replicate the kinematics of a ball and socket joint. Most importantly, the series of pin joints create two singularities, $180°$ apart from one another. These singularities can be moved, but cannot be eliminated.

Design of the elbow joint is considerably more straightforward because it can be approximated as a single pin joint. The actuator corresponding to this joint will incorporate a torque-limiting slip clutch, which decouples the actuator from the frame of the robotic arm if a predetermined torque value is exceeded. This device will help protect the user from injury by allowing free movement in the elbow if a spasm occurs in that joint.

The forearm roll will be the terminal joint on this prototype. It will be equipped with an encoder to measure the joint angle, but will not be driven. A mounting bracket for a hand grip will be rigidly attached to the forearm link through a six-axis force/torque sensor. Thus the wrist abduction and flexion joints will be fixed in the first hardware prototype.

B. Rapid-Prototyped Models

Two rapid-prototyped (RPT) models of the MGA Exoskeleton were built. The first prototype was used mainly to evaluate the kinematics and to decide what passive link adjustments would be required. The second prototype reflected kinematics changes following a design review and closely matched the final design. The prototypes were attached to the back of a neoprene *Uni-Vest* ^{TM} weight vest for portability, and a set of passive adjustments between the scapula and shoulder joints allowed for a customized fit.

1) Prototype I: A 3D model of the first prototype is shown in Figure 4. An adjustable linkage connects the scapulothoracic joint to the first shoulder pin joint which is oriented horizontally as seen in Figure 5. This segment has two angular adjustments accounting for curvature in the back, and a prismatic adjustment accounting for varying distance between the scalupo-thoracic joint and the GH joint.

The second joint axis was mounted orthogonally to the first, and the third joint axis was mounted orthogonally to the second. When the three GH joint axes become coplanar, the shoulder becomes singular. For an orthogonal triad, this singularity occurs when the first and third joint axes align producing a singularity along the direction of the first joint axis. The direction of this singularity can be changed using the second angular adjustment in the first linkage. Since this passive adjustment is oriented vertically, the singularity remains in the transverse plane.

The third GH joint axis is the shoulder internal/external rotation. A "C"-shaped linkage fits over the upper arm as shown previously in Figure 5. A strap secures a rotational joint on this linkage to the arm so that the joint moves with the arm. Modifications to the design of the first prototype began before the elbow linkage was constructed.

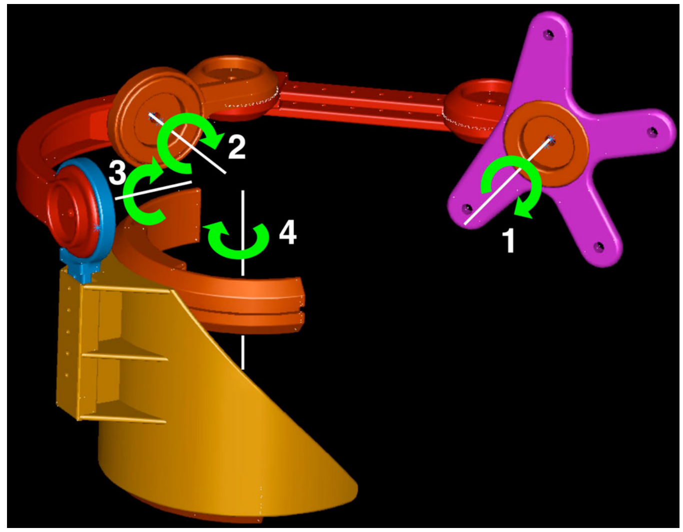

Fig. 4. CAD schematic of Prototype I.

Fig. 5. Side view of Prototype I with elbow and shoulder at $90°$ flexion.

2) Prototype II: A schematic of the second prototype is shown in Figure 6. Significant kinematic changes were implemented from the first prototype to move the singularity out of the transverse plane into a less intrusive location. As in the first prototype, an adjustable linkage connects the scapulothoracic joint to the first GH joint axis as seen in Figure 7. However, an additional passive rotation axis in the transverse plane is used to rotate the first shoulder axis (and thus singularity) about $30°$ from a normal to the plane containing the scapula axis and the GH joint.

Keeping the first axis away from the normal allows the arm to rest straight down against the side without being in a singular configuration. This alignment of the shoulder singularity with the azimuth axis in the *MB Exoskeleton* was very problematic during our examination (see Figure 2). Realignment of the azimuth axis was also employed in the *MULOS* design, although the tilt was 30° from vertical in the sagittal rather than frontal plane.

The second GH joint axis is oriented 90° from the first and is located to the side and slightly beneath the shoulder, as shown in Figure 7. The third GH joint is perpendicular to the second, but makes a 135°-angle with the first when the arm is in the rest position. The reason for making this angle 135° and not 90° is to allow the arm to abduct further before the first and third GH joints interfere with each other. Although the elbow linkage was not built for the prototype, the attachment to the upper arm can be seen at the base of Figure 7.

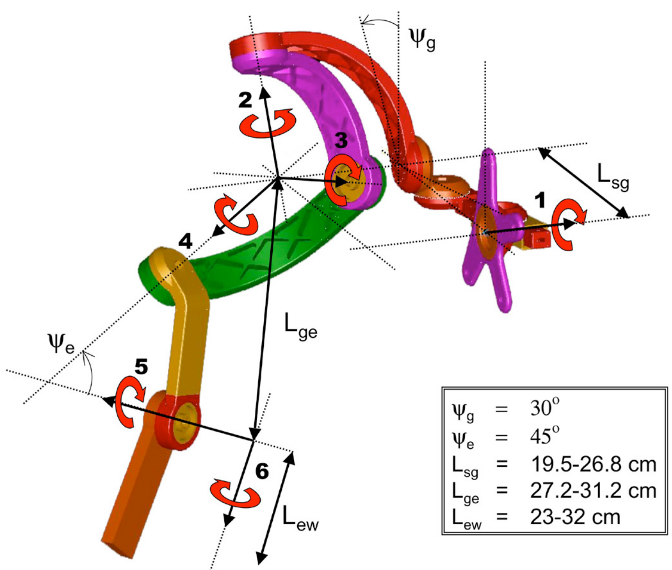

Fig. 6. CAD schematic of Prototype II.

C. Hardware

The objective of the mechanical design was to achieve at least half human strength and 90% of the human range of motion in each joint given previously in Tables II and III. The realized stall torque and range of motion for the active joints are given in Table IV and meet these specifications. A drawing of the final exoskeleton design is shown in Figure 8.

TABLE IV
JOINT CHARACTERISTICS FOR MGA EXOSKELETON.

Joint	Gear Ratio	Stall Torque (N-m)	Range (deg)
Scapula	160 : 1	92	$+30/-30$
GHR 1	160 : 1	92	$+180/-45$
GHR 2	160 : 1	92	$+90/-65$
GHR 3	160 : 1	92	$+210/-30$
Elbow	160 : 1	64	$+142/0$

Fig. 7. Prototype II is shown at 90° shoulder flexion while mounted to a weight vest.

Each joint (except for the forearm) is driven by a Kollmorgen brushless DC motor and harmonic drive transmission from HD Systems. Harmonic drives were chosen because of their compactness, low backlash, and backdrivability. The elbow is equipped with a slip clutch manufactured by Mayr Power Transmission and has an adjustable torque range of $20-50$ N-m. It also features a synchronous mechanism, which restricts the device from recoupling in all but one position, thus preserving the orientation between the input and the output.

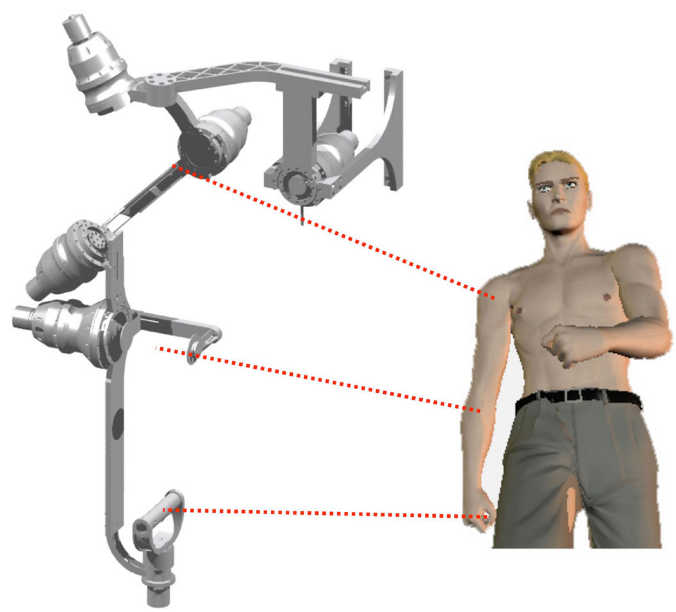

Fig. 8. IDEAS-CAD rendering of final exoskeleton design.

Power and communication is routed through an umbilical using a Galil 6-Axis Motion Control card mounted in the PC and Advanced Motion Control PWM power modules. Motor position is determined using an 1800-line optical incremental encoder manufactured by Numerik Jena. Single-turn, 12-bit optical absolute encoders manufactured by Gurley Precision Instruments are mounted at the output of the transmission to determine absolution position on start up and to monitor the incremental encoders.

A Model 50M31A force/torque sensor manufactured by JR3, Inc. is used to measure forces and torques on the handle. The sensor has a rating of 25 lb (111 N) in the radial direction and 50 lb (222 N) along the axial direction. The unit is a very compact 50 mm $\times$ 31 mm and has a mass of 0.15 kg. The sensor has integrated sensor electronics, and the six-channel digital output is read by a PCI card at 8 KHz. A single-axis torque sensor manufactured by Omega Engineering, Inc. is attached to the output side of the scapula transmission. The sensor is capable of measuring torque levels up to 113 N-m. Two single-axis compression load cells made by Sensotec, Inc. are attached to mounting plates on either side of the elbow to measure axial load at the elbow. Each sensor is capable of measuring forces up to 25 lb (111 N).

IV. Control System

The exoskeleton operates in two modes: Virtual Reality (VR) Mode and Physical Therapy (PT) Mode. In VR Mode, the forces exerted at the hand are controlled by interaction with a virtual environment generated by a computer. In PT Mode, the arm is allowed to rotate about an arbitrary axis through the shoulder using a preset resistance profile. In either mode, the scapula joint moves independently to "accommodate" the patient using sensed torque from the local torque cell. The control of the arm joints and scapula joint are described in more detail below.

A. Virtual Reality Mode

In Virtual Reality (VR) Mode, computer-generated environments are used to simulate daily living tasks for functionally-based rehabilitation. The patient views the simulated task and representation of their arm through a head mounted display while the exoskeleton provides haptic feedback to the patient. A force sensor located at the hand gripper senses the forces being exerted by the patient's "contact" with the virtual environment and relays them to the controller which moves the exoskeleton in response to the interaction.

Because the exoskeleton is kinematically redundant, specification of the wrist position is not enough to specify the three shoulder rotations and elbow pitch. This self-motion manifests itself as the ability of the elbow to "orbit" about the shoulder-wrist axis p_w shown in Figure 9 while the position of the wrist and shoulder are held fixed [14]. The angle formed by the shoulder-elbow-wrist (SEW) plane with a reference vector v is referred to as the "SEW angle."

The admittance controller shown in Figure 10 is used to convert the sensed contact forces at the hand and elbow into desired movements of the exoskeleton [7], [15]. Signals from the force-torque sensor at the hand are relayed to an admittance model of the virtual environment, which then outputs a desired

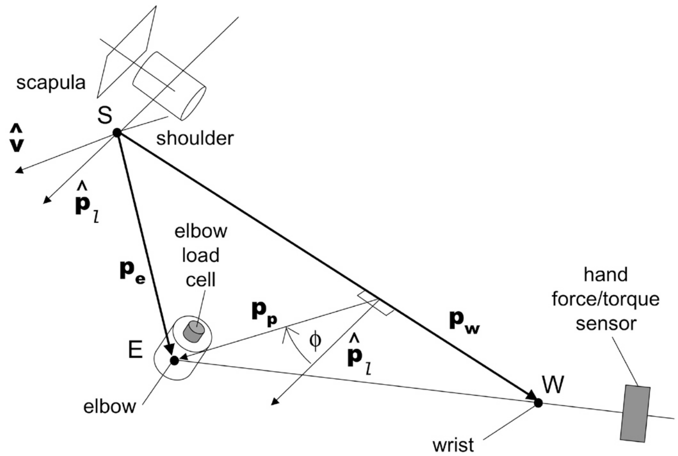

Fig. 9. Definition of shoulder-elbow-wrist (SEW) roll angle and location of gripper force/torque sensor and elbow axial load cells.

velocity for the wrist, $\dot{p}_w$. In addition, a pair of compression load cells mounted along the elbow axis are used to determine the torque, τ_ϕ, exerted about the shoulder-wrist axis, p_w. The SEW torque is then integrated to produce a desired SEW roll velocity $\dot{\phi}_d$ that is proportional to the torque about the p_w axis. The desired wrist and SEW velocities are then converted to desired angular velocities at the joints using the inverse Jacobian, $J_{w\phi}$, and the resultant desired joint angles, $\dot{\theta}_d$, are then tracked using a proportional-derivative (PD) control law.

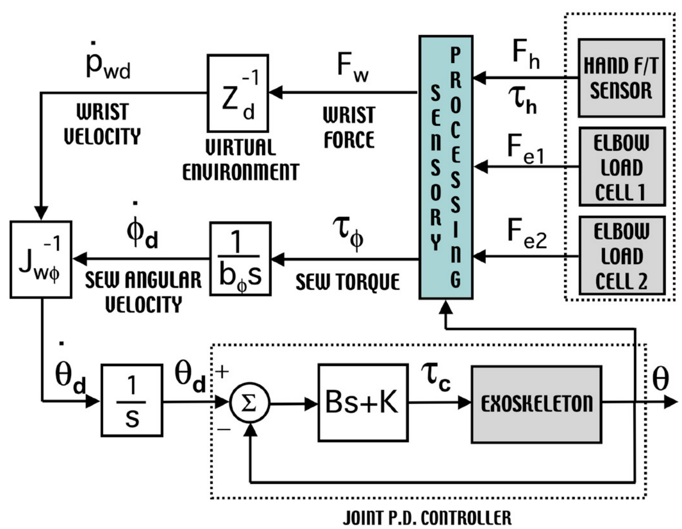

Fig. 10. Admittance controller used in VR Mode.

B. Physical Therapy Mode

In Physical Therapy (PT) Mode, the exoskeleton becomes a programmable resistance trainer that allows the patient to exercise about an arbitrary shoulder rotation axis. For rotator cuff injuries, for example, therapists often prescribe exercises involving lateral/medial rotation of the shoulder. Since there is no single joint corresponding to shoulder rotation, the exercise involves all three shoulder axes of the exoskeleton. Thus, the controller needs to yield a prescribed resistance profile about the desired axis while preventing rotations about the other shoulder axes.

Since the torques about the shoulder axes cannot be measured directly, an impedance controller is used to realize the desired resistance profile [17]. The shoulder joint velocities are relayed to a Jacobian, J_{GH}, as shown in Figure 11, which then computes the Cartesian velocities about the glenohumeral (GH) joint, ω_{GHd}. These velocities are then multiplied by the desired resistance profile, which outputs the desired torques about the GH axes, τ_{GHd}. These torques are then converted into exoskeleton joint torques using the Jacobian. A feedforward model of the exoskeleton runs in parallel to calculate gravity and other feedforward compensation torques. Since only the GH angles are specified, the elbow pitch is left unconstrained and can be moved however the patient desires.

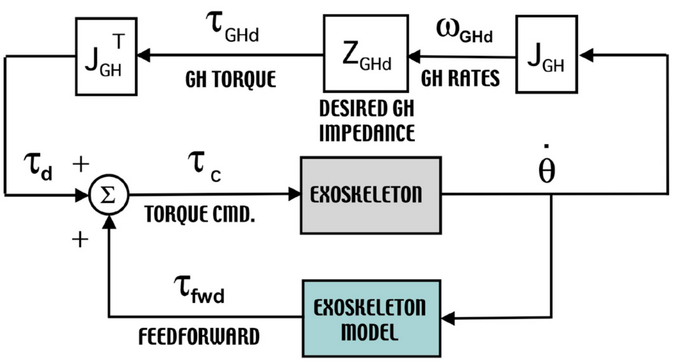

Fig. 11. Impedance Controller used in PT Mode.

C. Scapula Joint Control

The scapula joint is controlled independently from the arm joints using the admittance controller shown in Figure 12. A torque cell at the output of the transmission directly measures the torque being exerted by the scapula joint, τ_{ξ}. However, because the applied torque must balance the sum of the gravitational torque and the torque applied by the subject, a gravitational model is used to subtract out the component due to the gravity load. The estimated human torque is then integrated to produce a desired scapula joint velocity, $\dot{\xi}_d$, which is then tracked by a PD controller.

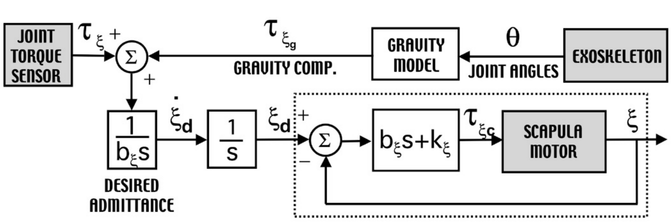

Fig. 12. Accommodation controller used for scapula joint.

V. Software Architecture

The architecture of the control system is shown in Figure 13. The health worker interacts with the system through the control station and its user interface. This interface allows the clinician to monitor the robotic system performance, enter patient rehabilitation parameters, and store patient history. The control station communicates over the Internet with the robot control computer, which is responsible for control of the robotic arm and overall patient safety. The arm controllers running on the robot control computer produce either a position or torque command, which is sent to the motor controller. A force-torque sensor attached to the gripper senses the forces and torques exerted by the patient, which are relayed to the robot control computer via a digital acquisition board.

The robot control computer runs the TimeSys Linux realtime operating system, in order to guarantee meeting its safety deadlines. As the operator computer is not involved in safety decisions, it will run a standard desktop operating system (in which the ability to respond to events within a certain time frame is not guaranteed). The arm controller algorithms operate in Cartesian space, utilize force/torque sensor data, and operate at 200 Hz. The PD controller, when required by a particular arm controller, runs at 1000 Hz.

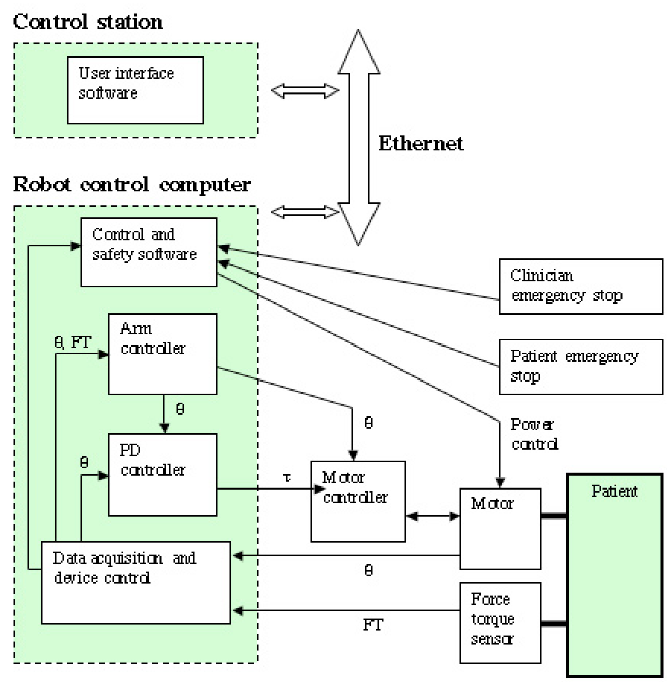

Fig. 13. Software control architecture.

All safety decisions are carried out within the robot control computer and occur autonomously. This setup allows for very high speed reaction by the computer safety system in the event of a component failure, communication error, or the patient attempting something they should not. The embedded robot system is designed to be a 'fail-safe' system, and is, as much as practical, safe in and of itself. The actual 'safe state' entered will be one of: a) the arm holding its current position and not exerting any force on the patient, or b) a complete power-down of the arm. At any time, either the clinician or the patient are able to manually safe the system by hitting a button or key.

The robot control computer is responsible for enforcing patient-related force, position, and range-of-motion limits; guaranteeing that the heartbeat transmitted by every computer is valid; verifying that all the local electronics are functioning and correctly providing data; and ensuring that the operator computer is functioning. These checks occur at either 200 or 1000 Hz, depending on whether they are associated with the arm or PD controller. Also, the robot control computer is protected by watchdog timers that will safe the system in the event of incorrect operation.

The reaction time of the software safety system determines how much affect a failure can have on the patient, in terms of how much additional force can be applied or how far the arm can move, before the system safes. This effect depends on the reaction time of the robot control computer and the rate of the particular safety check. As software checks are executed at either 200 or 1000 Hz, the reaction time will be a maximum of 5 ms, and a minimum of 1 ms.

VI. Conclusion

This paper began with a survey of exoskeletons built to-date and has explored the design tradeoffs between various kinematic designs and actuator technologies. Only one exoskeleton was found that incorporated scapulothoracic motion, but it was not powered. A single rotary joint perpendicular to the back was chosen to accommodate shoulder elevation and depression. The glenohumeral joint is based on an orthogonal axis triad with the first axis tilted at $30°$ away from the azimuth axis to accommodate the singularity. Two rapid-prototyped versions of the exoskeleton were built prior to final design. Mechanical fabrication is complete, and the exoskeleton is now undergoing electronics integration and testing. Although the prototype mass is only about 12 kg, it will initially be wall-mounted due to the weight of the external components.

Acknowledgment

Thanks go to the rest of the team, Brian, Walt, Jean-Marc, and John, and also to Jeff, Amanda, and Brooke for test-fitting the prototypes. We are also grateful to Kevin McQuade and Matt Elrod for their helpful insights on shoulder rehabilitation, and Daniel Repperger of Wright-Patterson AFB for letting us examine the MB Exoskeleton. This project is being sponsored by the U.S. Medical Research and Materiel Command under Grant #DAMD17-99-1-9022.

References

[1] K. N. An, L. J. Askew, and E. Y. Chao, "Biomechanics and functional assessment of upper extremeties," in *Trends in Ergonomics/Human Factors III*, W. Karwowski, Ed. North-Holland: Elsevier Science Publishers B. V., 1986.

[2] M. Bergamasco, B. Allotta, L. Bosio, L. Ferretti, G. Parrini, G. Prisco, F. Salsedo, and G. Sartini, "An arm exoskeleton system for teleoperation and virtual environments applications," in *Proc. of the IEEE Intl. Conf. on Robotics and Automation*, San Diego, 1994, pp. 1449–1454.

[3] M. A. Buckley and R. R. Johnson, "Computer simulation of the dynamics of a human arm and orthosis linkage mechanism," in *Proc. Instn. Mech. Engrs. Part H*, vol. 211, 1997, pp. 349–357.

[4] G. C. Burdea, *Force And Touch Feedback For Virtual Reality*. New York: John Wiley and Sons, 1996.

[5] D. G. Caldwell, C. Favede, and N. Tsagarakis, "Dextrous exploration of a virtual world for improved prototyping," in *Proc. of the IEEE Intl. Conf. on Robotics and Automation*, leuven, belgium, may 1998, pp. 298–303.

[6] D. G. Caldwell, O. Kocak, and U. Andersen, "Multi-armed dexterous manipulator operation using glove/exoskeleton control and sensory feedback," in *Proc. of the IEEE/RSJ Intl. Conf. on Intelligent Robots and Systems*, pittsburg, USA, Aug. 1995, pp. 567–572.

[7] C. Carignan and D. Akin, "Achieving impedance objectives in robot teleoperation," in *Proc. of the IEEE Conference on Robotics and Automation*, 1997, pp. 3487–3492.

[8] W. Chou and T. Wang, "Haptic interaction with virtual environment using an arm type exoskeleton device," in *Proc. of the IEEE Intl. Conf. on Robotics and Automation*, new orleans, USA, apr 2004, pp. 1992–1997.

[9] H. P. V. Cott and e. Robert G. Kinkade, *Human Engineering Guide to Equipment Design, rev. ed.* New York: McGraw-Hill, 1963.

[10] R. L. W. II, M. A. Murphy, D. North, J. Berlin, and M. Krier, "Kinesthetic force/moment feedback via active exoskeleton," in *Proc. of the Image Society Conference*, scottsdale, arizona, 1998.

[11] S. C. Jacobsen, F. M. Smith, and D. K. Backman, "High performance, dextrous telerobotic manipulator with force reflection," in *Intervention/ROV'91 Conference and Exposition.* Hollywood, Florida: Marine Technology Society, May 1991, pp. 213–218.

[12] G. R. Johnson, D. A. Carus, G. Parrini, S. S. Marchese, and R. Valeggi, "The design of a five-degree-of-freedom powered orthosis for the upper limb," in *Proc. Instn. Mech. Engrs. Part H*, vol. 215, 2001, pp. 275–284.

[13] E. Kreighbaum and K. M. Barthels, *Biomechanics: a qualitative approach for studying human movement, 4th Ed.* Boston: Allyn and Bacon, 1996.

[14] K. Kreutz-Delgado, M. Long, and H. Seraji, "Kinematic analysis of 7 dof manipulators," *Int. Journal of Robotics Research*, vol. 11, no. 5, pp. 469–481, 1992.

[15] J. Maples and J. Becker, "Experiments in force control of robotic manipulators," in *Proc. of the IEEE Conference on Robotics and Automation*, Apr. 1986, pp. 695–702.

[16] S. Marcheschi, "Progettazione e realizzazione di un sistema di controllo per uninterfaccia aptica a 7 gradi di libert," Master's thesis, Università Degli Studi Di Pisa, apr 2001.

[17] T. Massie and J. K. Salisbury, "The PHANTOM haptic interface: A device for probing virtual objects," in *Proc. ASME Winter Annual Meeting: Symposium on Haptic Interfaces for Virtual Environment and Teleoperator Systems*, Nov. 1994.

[18] E. J. McCormick, Ed., *Human Factors Engineering, 3rd ed.* New York: McGraw-Hill, 1970.

[19] T. B. Moeslund, C. B. Madsen, and E. Granum, "Modelling the 3d pose of a human arm and the shoulder complex utilising only two parameters," in *Proc. of the Intl. Conference on Model-based Imaging, Rendering, Image Analysis and Graphical Special Effects*, INRIA Rocquencourt, France, 2003.

[20] A. Nakai, Y. Kunii, H. Hashimoto, and F. Harashima, "Arm type haptic human interface: Sensor arm," in *Intl. Conf. on Artificial Reality and Tele-Existence (ICAT)*, Tokyo, Japan, Dec. 1997, pp. 77–84.

[21] A. Nakai, T. Ohashi, and H. Hashimoto, "7 dof arm type haptic interface for teleoperation and virtual reality systems," in *Proc. of the IEEE/RSJ Intl. Conf. on Intelligent Robots and Systems*, Victoria, B.C., Canada, Oct. 1998, pp. 1266–1271.

[22] D. W. Repperger, S. J. Remis, and G. Merrill, "Performance measures of teleoperation using an exoskeleton device," in *Proc. of the IEEE Intl. Conf. on Robotics and Automation*, Cincinnati, May 1990, pp. 552–557.

[23] D. P. Romilly, C. Anglin, R. G. Gosine, C. Hershler, and S. U. Raschke, "A functional task analysis and motion simulation for the development of a powered upper-limb orthosis," *IEEE Transactions on Rehabilitation Engineering*, vol. 2, no. 3, pp. 119–129, Sept. 1994.

[24] J. Rosen, B. Hannaford, and S. Burns, "Neural control of an upper limb powered exoskeleton system – grant report," in *Proc. of the First NSF Robotics and Computer Vision (RCV) Workshop*, Los Vegas, Oct. 2003.

[25] N. Tsagarakis, D. G. Caldwell, and G. A. Medrano-Cerda, "A 7 dof pneumatic muscle actuator (pma) powered exoskeleton," in *Proc. of the IEEE Intl. Workshop on Robot and Human Interaction*, Pisa, Italy, sep 1999, pp. 327–333.

[26] Y. Umetani, Y. Yamad, T. Morizono, T. Yoshida, and S. Aoki, "*Skil Mate*, wearable exoskeleton robot," in *Proc. of the IEEE Intl. Conf. on Robotics and Automation*, 1999, pp. 984–988.